

# MULTI-ANGLE MONITORING OF DESERT DUNE TOPOGRAPHY

Ji Ye, Yun<sup>1</sup> Jung Rack, Kim\*<sup>2</sup> Yun Soo Choi<sup>3</sup>

<sup>1</sup>Graduate Student, Department of Geoinformatics, University Of Seoul  
*Seoulsiripdaero 163., Dongdaemum-gu, Seoul,130-743, Korea; Tel: + phone (+82) 0222105073*  
E-mail: jy01@uos.ac.kr

<sup>2</sup>Research Professor, Department of Geoinformatics, University Of Seoul  
*Seoulsiripdaero 163., Dongdaemum-gu, Seoul,130-743, Korea; Tel: + phone (+82) 07082533008*  
Email: kjrr001@gmail.com

<sup>3</sup>Professor, Department of Geoinformatics, University Of Seoul  
*Seoulsiripdaero 163., Dongdaemum-gu, Seoul,130-743, Korea; Tel: + phone (+82) 0222105073*

**KEY WORDS:** Desert dune, MISR, Dust storm, Local roughness

**ABSTRACT:** The global desert coverage has been rapidly expanding due to the reasons such as climate change and uncontrolled human activities. Thus, the importance of the observation tool not only for the growth of desert but also for the sandy dune activity has been recently noticed. In this study, we developed the monitoring methods of sand dune field by the Multi angle imaging Spectro Radiometer (MISR). Normalized Difference Angular Index (NADI) extraction was proposed as the main idea tracing the sandy desert because of its obvious correlation with the local roughness properties of the sandy dunes fields. For the test areas in Kubuchi and Badein deserts in northwest China, the spatial and temporal transitions were well identified employing the scheme based on MISR NDAI. The algorithms to measure the magnitude of sand dune migration will be further developed.

## 1. Introduction

The increasing occurrences of mineral dust storm become a serious threat in human activities as well as public health over Far East Asian area. The interpretation by the MODIS analysis (Zhang et al., 2007) and the particle trajectory simulation with HYSPLIT (HYbrid Single-Particle Lagrangian Integrated Trajectory) (Kim et al., 2011) identified the sandy deserts in northwest China as the primary source of mineral aerosol. Since the sand dune activity in the desert terrain has been recognized as an essential indicator of the mineral aerosol generation, it is important to monitor the extents and the variations of the specific topographic properties such as local roughness of sand dune field.

Especially, it is well known the aerodynamic roughness lengths  $Z_0$  which can be driven from the specialized sensor such as POLDER (POLarization and Directionality of the Earth's Reflectances) is essential to understand desert dune characteristics (Marticorena et al., 2004). However, even with long term observation over dune fields, the data coverage for the extraction of  $Z_0$  is limited. Therefore, MISR image sequence was employed to extract the simple multi angle topographic parameters such as NDAs instead of  $Z_0$ . The multi angle observation showed a correlation between the intensities and the extents of sand dune activities and the climate condition in the aerosol source areas. The tracing results in northwest China by MISR NDAs were demonstrated in this study.

## 2. Background

A research by Tegen and Fung (1995) estimated that 30-50% of mineral aerosol is originated from the sandy desert. The emission mechanism of mineral aerosol over the sandy desert during the dust storm period as a typical land-atmospheric interaction, are not well known. The model establishments by the simulations of dust emission processes using synoptic meteorology have been continuously failed because of the insufficient information about topographic conditions (Marticorena et al., 2004). In very rough description, the saltation process which is the main driving force of the dune migration makes the suspension of some particles. After then, the particle moves beyond the local area under the specific climate condition. As the primary parameter in the process is the aerodynamic roughness length  $Z_0$  governing whole dust emission mechanism,  $Z_0$  is highly important for the identification of aeolian places, for example sandy desert, as well as the characterization of the surface condition.

In spite of its importance, the direct measurement of  $Z_0$  over the target surfaces is hardly feasible so that the alternative local roughness parameters from medium resolution satellite imagery which can be calibrated into  $Z_0$  should be devised. Then the distribution of the local roughness parameter and the extent of sandy desert are able to be crossly investigated.

### 2.1 Local roughness parameter

A well known multi angle approaches for the local roughness extraction is the establishment of Hapke reflectance function and the inversion of roughness parameters from the fitted model (Hapke, 1993). It has been usually employed for the investigation of microscopic properties of regolith. The effectiveness for the large scale geomorphic feature analysis was also demonstrated in Wu et al., (2008)'s work over dune fields. However, the multiple optical imaging for Hapke modeling over target surface is not usually feasible. Hence, the simplified methods with multi angle imaging are required.

Two alternative approaches were proposed. The one is the two-look surface roughness extraction proposed by Muskin and Gillespie (2005). The method is the simple division of the co-registered pixel radiances in two look optical channels. Then the ratio of two pixels is

$$\frac{R_{sensor1}}{R_{sensor2}} = \frac{\frac{1}{\pi} I_1 \tau_{sun1} \tau_{sensor1} \rho_1 (1 - f_{shadow1})}{\frac{1}{\pi} I_2 \tau_{sun2} \tau_{sensor2} \rho_2 (1 - f_{shadow2})} \quad (1)$$

where  $R_{sensor1,2}$  is the measured radiance of multi angle channel 1 and 2,  $I$  is solar irradiance at top of atmosphere,  $\tau_{sun}$ ,  $\tau_{sensor}$  are atmospheric transmissivity in the sun and sensor surface paths,  $\rho$  is the surface reflectivity and  $f_{shadow}$  is the effective fraction of the pixel area that is in shadow. In here the all terms except  $f_{shadow}$  are canceled out or remain constant across the scene as long as the pixels in channels are correctly registered. Then the radiance ratio depends on the surface roughness. After examining the idea with ASTER (Advanced Spaceborne Thermal Emission and Reflection Radiometer) over terrestrial surface, they applied the method for the THEMIS (Thermal Emission Imaging System) two look images and HRSC stereo channels in S1 and S2 (Muskin and Gillespie, 2006) over martian surface.

The similar but advanced concept so called Normalised difference Angular Index (NDAI) to extract local roughness from multi angle observation was introduced by Nolin et al., (2002) for MISR (Multi-angle Imaging Spectro Radiometer) image. The NDAI can be express as

$$NDAI = \frac{R_{forward} - R_{backward}}{R_{forward} + R_{backward}} \quad (2)$$

where  $R_{forward, backward}$  is the bidirectional reflectance (BRF) on the top of atmosphere (TOA) of forward and backward channels which have up to 60 degree view angles in the case of MISR. In the similar way with the two look approach, NDAI retains the effects of non-shadow fraction of pixels. Nolin and Payne (2007) used NDAI to measure the local roughness of sea ice and glacier. Considering the sandy desert dunes have less 3D variation than the vegetation canopy in the meter scale, NDAI over the sandy dune fields should be clearly lower than any other topographic surfaces.

## 2.2 Study Area and sensor

Western China has been suffering by the heavily desertification, even though Wang et al., (2006,2009) recently reported the dune activities in China are ceasing. A good example is Kubuchi and Badaian Jaran desert area in Nei-Mongolia where a combat desertification activity by Korea-China NGO alliance is undergoing. Combining HYSPLIT simulation results with the dust storm trails from MODIS multi spectral analyses, 67% of dust storm over Far East Asia were traced in this area (Kim et al., 2011). Together with such significant contribution in dust storm cycle and the rapid transition between desert and soil, this area was chosen as the test site of our monitoring scheme.

The primary sensor to monitor the sandy desert is MISR designed for the better understanding of Earth environment. The instrument was optimized for the multi angular measurements to obtain angular reflectance which is essential for the extraction of roughness parameters

## 3. Results

MISR were equipped with the five channels in different view angles- i.e.  $0^\circ$ ,  $26.1^\circ$ ,  $45.6^\circ$ ,  $60.0^\circ$ , and  $70.5^\circ$ , so called An, Af/Aa, Bf/Ba, Cf/Ca, and Df/Da, respectively. In order to observe more comprehensive surface roughness, NADI values in all four channel combinations were extracted. Then the surface micro scale properties were more clearly identified in four different NDAI channels. In general, the desert dune has highly smooth surface in micro scales due to the continuous interaction between the surface wind and the sand particles. Therefore the four NDAIs were expected to show consistently lower values compared the other landcover types.

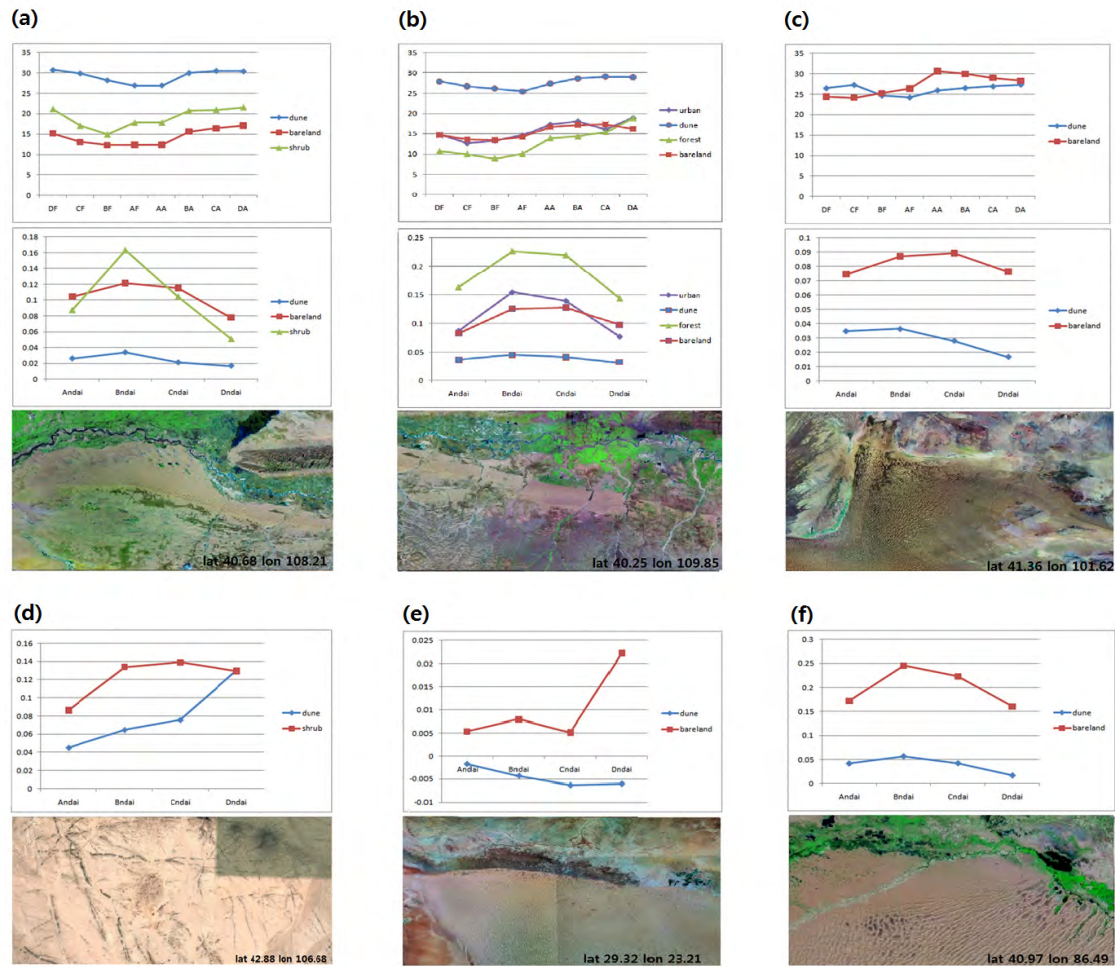


Figure 1. NDAI distributions over testing sites, (a) BRF and NDAI values in Kubuchi desert, (b) BRF and NDAI values in eastern Kubuchi desert (c) BRF and NDAI values in Badian Jaran desert, (d) NDAI values in Gobi rocky desert, (e) NDAI values in Sahara desert, (f) NDAI values in Taklomakan Desert

### 3.1 NDAI sampling over test areas

Those assumptions about NDAI were tested in the several sample areas. Figure 1 showed the NDAI and reflectance values in Badian Jaran (c), Kubuchi (a)-(b), Gobi (d), Eastern Sahara (e) and Taklomakan Desert (f) respectively. All sandy dune fields showed consistently low values in four NDAI channels while any distinguished reflectance difference from the other landcover classes was not founded. Considering that only Gobi desert has rocky surface, the NDAI distribution in Gobi desert as shown in Figure 2 (d) was likely originated from its unique surface characteristics. Since the micro scale roughness in rocky surface is clearly higher than the sandy particle structures, the relatively high NDAI values in Gobi desert can be explained accordingly.

Especially an interesting fact is the anomalous NDAI values in Sahara desert. It is still lower than the NDAI value in the surrounding barren field but showed the different variation in viewing channels compared with the other deserts. The reason of such NDAI behavior might be the different dune shape from the other testing areas. The target area in Sahara desert is covered by the star type sand dune originated by indigenous environments. It produces the different irradiance according to the viewing geometry and the illumination condition and affects the distribution of NDAI values significantly.

Overall, owing to the consistently low values and the variation pattern in all viewing channels, the NDAI in desert demonstrated the full potential to classify the sandy desert from the other landcover types.

### 3.2 The sandy desert tracing with MISR NDAIs

Based in all above assessment results, the scheme to trace the sandy desert boundary using NDAIs was designed. The main idea of the desert boundary tracer is the spatial restriction of the sandy desert transition area. Most likely, the transition between the sandy dune field and the other landcover types occurred only in the edge of desert. Therefore, the multi temporal MISR images were processed by the feed-forward classifier scheme combining the

morphological filtering. In detail, four MISR NDAIs channels of initial observation time were classified with the SVM (Support Vector Machine) algorithms. To prevent the miss-classification, only three landcover types, i.e., non-desert, sandy desert and water, were introduced. Especially it should be noted the water type in classification scheme is essentially necessary because the water is the most “gentle” surface among all the natural topographies so that the high similarity between NDAI values of water and sandy desert exists. After then the classification result from the first output was feed forward to the next image in time sequence applying the morphological filtering in order to split the edge parts which can be more likely transfer to the other landcover types. The delivered classification result was then used as the training data in the next processing scheme. Such processing stage was conducted through the whole multi temporal images so that the desert coverage in the multi temporal MISR NDAI images was successfully reconstructed.

Figure 2 showed the sandy desert boundaries in western China including Badein Jaran and Kubuchi desert during 2000-2008 period. MISR image mosaics were used to cover whole wide areas. The problem of image irradiances normalization over the mosaic image coverage was naturally addressed owing to the introduction of NDAIs.

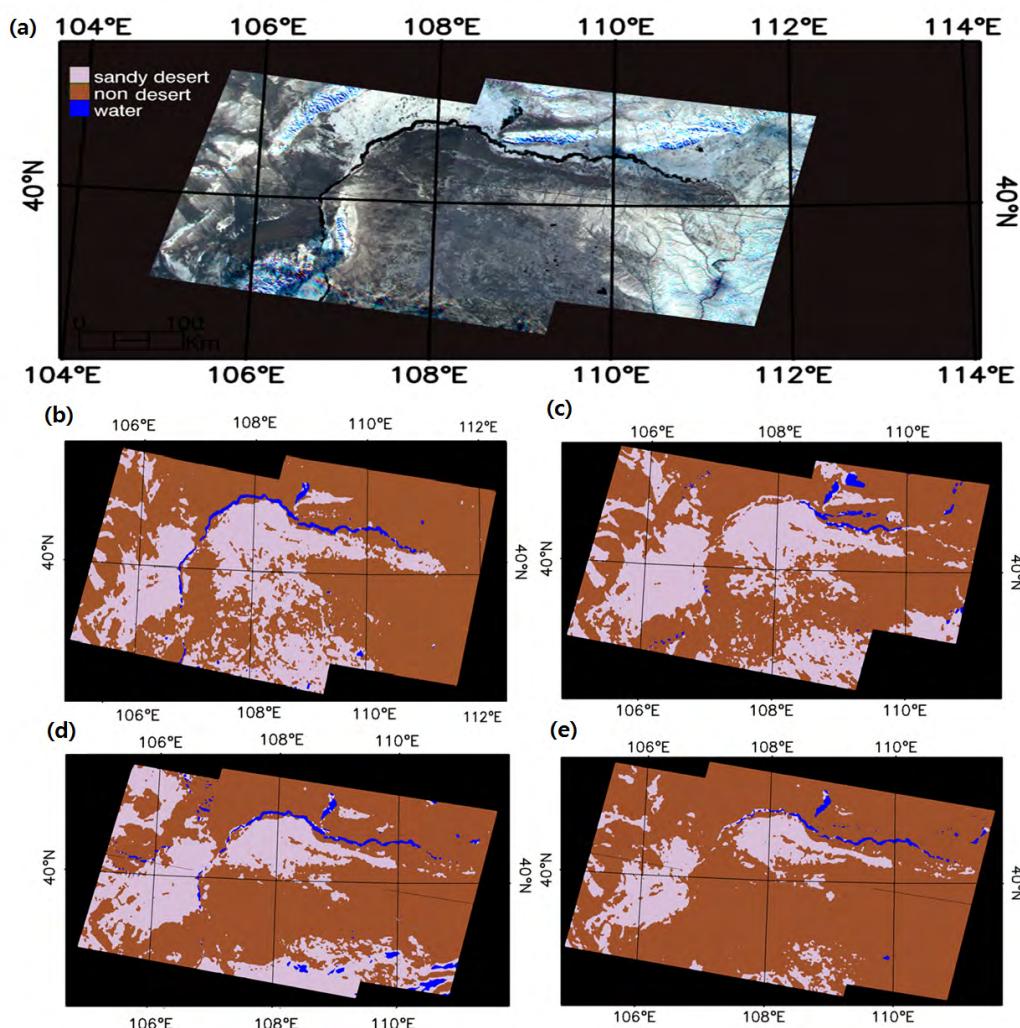


Figure 2. The sand dune boundaries tracing in western China, (a) the color composite image of in 2000 MISR NDAI mosaic (R: Ba/Bf, G: Ca/Cf, B: Da/Df NDAI) (b) the sandy desert boundary in 2000, (c) the sandy desert boundary in 2001, (d) the sandy desert boundary in 2004, (e) the sandy desert boundary in 2008

The color composite in Figure 2 (a) demonstrated the solid bases of the NDAI employment for the desert boundary tracing. The dark desert areas where all NDAI channels have low values are clearly distinguished and reveal the different pixel properties from the water surface. On the contrary, all light tone areas where the surface is consistently rough in NDAI measurements can be easily managed by the classification scheme. After all, the desert boundary in Figure 2 (b) were correctly identified and provided the high accuracy training data for the next MISR NDAI images as shown in Figure 2 (c)-(e).

Figure 3 showed the processing results with single MISR NDAI coverage over the eastern Kubuchi area where the combat desertification activities are mainly conducted. Compared with the color composite images, the high accuracy desert boundaries were extracted over test areas.

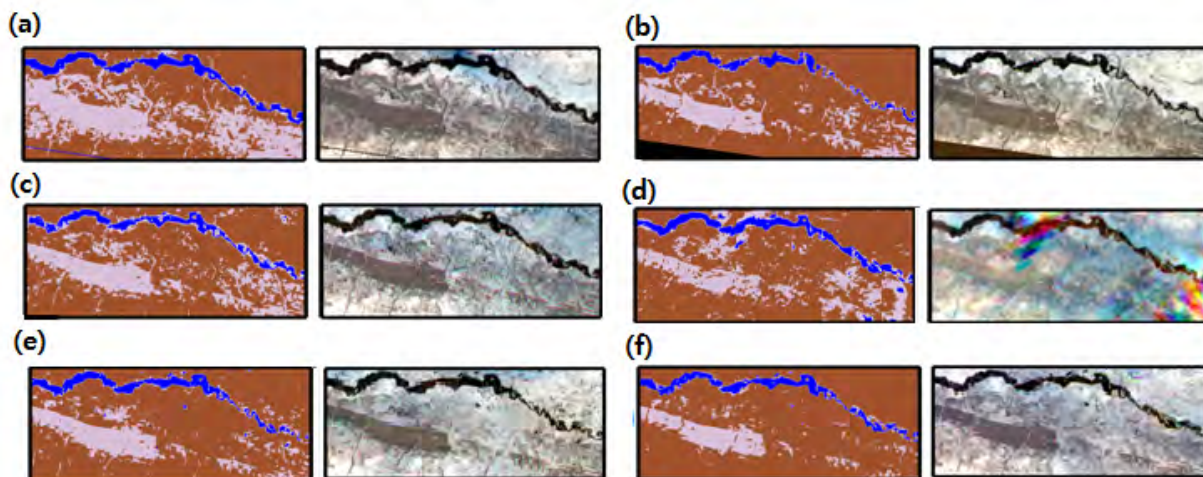


Figure 3. The sand dune boundaries tracing in Kubuchi desert, (a) the sandy desert boundary (left) and the RGB color composites of NDAI channels (right) in 2000 (b) the sandy desert boundary in 2001, (c) the sandy desert boundary in 2005, (d) the sandy desert boundary in 2006, (e) the sandy desert boundary in 2008, (f) the sandy desert boundary in 2009

#### 4. Conclusion

In this study, we proved the effectiveness of MISR NDAIs to trace and identify the sandy desert. The results coincided with the assumption that the sandy dune migration by the surface wind cause very smooth surface in micro scales.

Especially an interesting fact from our analysis is the degeneration of sandy desert in western China for last a decade, even though the sandy desert boundaries can make the local variation according to the temporal climate condition. It should be noted that the other research and the ground observation by the acting agencies in the combat desertification in this area also proposed the gradual reduction of the sandy desert.

Actually, the landcover classification with high and very high resolution imagery can provide the desert boundary with better accuracy. However, the total costs and time to acquire the high and very high resolution images for the whole coverage in target desert are not manageable. As the other possible replacement by 1km resolution global landcover class from MODIS imagery is not suitable because of its large spatial resolution, the desert tracing scheme employing MISR NDAIs have the clear superiority in the aspect of accuracy and spatial resolution (<500m).

In future, the variation of multi angle observation over potential dust source area combining with the metrological observations will be traced as a next topic. If the correlation between the intensities and the extents of sand dune activities and the surface wind conditions in the aerosol source areas is identified, it will give a highly important clue for the understanding of the dust storm generation process.

#### Acknowledgements

The authors acknowledge Future Forest and United Nations Convention to Combat Desertification for supporting this study. The first and third authors' researches in this study were supported by Project to Educate GIS Experts.

#### 6. Reference

- Hapke, B.W., 1993. Theory of reflectance and Emittance Spectroscopy. Cambridge Univ. Press, New York.
- Kim, J. R., Yun, J., Choi, Y.S. and Yun, H.W., 2011. The correlation analysis between the dust storm in Far East Asia and the dynamic local roughness in northwest China sandy desert by remote sensed data. EGU 2011
- Marticorena, B., and G. Bergametti, 1995. Modeling the atmospheric dust cycle: 1. Design of a soil derived dust production scheme. Journal of Geophysical Research, 100 (16),pp.415-430.
- Marticorena, B., P. Chazette, G. Bergametti, F. Dulac, and M. Legrand, 2004. Mapping the aerodynamic roughness length of desert surfaces from the POLDER/ADEOS bi-directional reflectance product. International Journal of Remote Sensing, 25(3), pp.603– 626.

- Marticorena, B. Kardous, M. Bergametti, G. Callot, Y. Chazette, P. Khatteli, H. Le Hegarat-Mascle, S. Maille, M. Rajot, J.-L. Vidal-Madjar, D., 2006. Surface and aerodynamic roughness in arid and semiarid areas and their relation to radar backscatter coefficient. *Journal of Geophysical Research*, 111, F03017, doi:10.1029/2006JF000462.
- Mushkin, A., and Gillespie, A. R., 2005. Estimating sub-pixel surface roughness using remotely sensed stereoscopic data, *Remote Sensing of Environment*, 99, pp.75 – 83.
- Mushkin, A., and Gillespie, A. R., 2006. Mapping sub-pixel surface roughness on Mars using high-resolution satellite image data, *Geophysical Research Letter*, 33, L18204.
- Nolin, A. W., Fetterer, F. M., and Scambos, T. A., 2002. Surface roughness characterizations of sea ice and ice sheets: Case studies with MISR data. *IEEE Transaction on Geoscience and Remote Sensing*, 40(7), pp.1605–1615.
- Nolin, A. W., and Payne, C. M., 2007. Classification of glacier zones in western Greenland using albedo and surface roughness from the Multi-angle Imaging SpectroRadiometer (MISR). *Remote Sensing of Environment* 107, pp. 264–275 .
- Tegen, I. and I. Y. Fung, 1995. Contribution to the mineral aerosol load from land surface modification. *Journal of Geophysical Research*, 100(18) ,pp.707-726.
- Wang X., Hasi E., Zhou Z., and Liu X., 2006. Significance of variations in the wind energy environment over the past 50 years with respect to dune activity and desertification in arid and semiarid northern China. *Geomorphology*, 86, pp.252-266.
- Wang X., Yang Y., Dong Z., and Zhang C., 2009. Responses of dune activity and desertification in China to global warming in twenty-first century. *Global and Planetary Change*, 67, pp.167-185.
- Wu, Y., Gong, P., Liu, Q. and Chappell, A., 2009. Retrieving photometric properties of desert surfaces in China using the Hapke model and MISR data. *Remote Sensing of Environment*, 113 (1), pp. 213-223.
- Zhang B., Tsunekawa A., and Tsubo M., 2008. Contributions of sandy lands and stony deserts to long-distance dust emission in China and Mongolia during 2000–2006. *Global and planetary change*, 60, pp.487-504.